Multivalent Mechanism of Membrane Insertion by the FYVE Domain*⑤

Tatiana G. Kutateladze‡§, Daniel G. S. Capelluto‡, Colin G. Ferguson¶, Matthew L. Cheever‡‖, Andrei G. Kutateladze**, Glenn D. Prestwich‡‡, and Michael Overduin‡

*From the ‡Department of Pharmacology and the ‖Molecular Biology Program, University of Colorado Health Sciences Center, Denver, Colorado 80262, ¶Echelon Biosciences Inc., Salt Lake City, Utah 84108, the **Department of Chemistry and Biochemistry, The University of Denver, Denver, Colorado 80210, and the ‡‡Department of Medicinal Chemistry, The University of Utah, Salt Lake City, Utah 84108*

Targeting of a wide variety of proteins to membranes involves specific recognition of phospholipid head groups and insertion into lipid bilayers. For example, proteins that contain FYVE domains are recruited to endosomes through interaction with phosphatidylinositol 3-phosphate (PtdIns(3)P). However, the structural mechanism of membrane docking and insertion by this domain remains unclear. Here, the depth and angle of micelle insertion and the lipid binding properties of the FYVE domain of early endosome antigen 1 are estimated by NMR spectroscopy. Spin label probes incorporated into micelles identify a hydrophobic protuberance that inserts into the micelle core and is surrounded by interfacially active polar residues. A novel proxyl PtdIns(3)P derivative is developed to map the position of the phosphoinositide acyl chains, which are found to align with the membrane insertion element. Dual engagement of the FYVE domain with PtdIns(3)P and dodecylphosphocholine micelles yields a 6-fold enhancement of affinity. The additional interaction of phosphatidylserine with a conserved basic site of the protein further amplifies the micelle binding affinity and dramatically alters the angle of insertion. Thus, the FYVE domain is targeted to endosomes through the synergistic action of stereospecific PtdIns(3)P head group ligation, hydrophobic insertion and electrostatic interactions with acidic phospholipids.

Cellular processes including signal transduction, vesicular trafficking, and cytoskeletal rearrangement require selective recruitment of proteins to membrane surfaces. Well established mechanisms for localizing cytosolic proteins to membranes include electrostatic interactions through a basic peptide sequence, anchoring by covalently attached acyl chains, and association with the cytoplasmic domains of transmembrane proteins (reviewed in Refs. 1 and 2).

The recognition of phosphoinositide (PI)[1] head groups by conserved structural domains has recently emerged as another major membrane targeting mechanism. Seven differentially phosphorylated PIs are bound by protein modules including the C2, ENTH, FERM, FYVE, PH, PX, SH2, and Tubby domains (reviewed in Ref. 3), as well as the BAR (4), PDZ (5), and PTB (6) domains. Although the majority of these domains can interact with several PIs, the FYVE domain is remarkably selective for PtdIns(3)P (7–9). In addition to PI ligation, these domains often insert hydrophobic elements into the membrane bilayer, as has been demonstrated for the C2 (10), ENTH (11), FERM (12), FYVE (13), and PX (14) domains and the vinculin tail (15). Insertion into the membrane can be accompanied by interactions with multiple lipid head groups. For example, the PX domain of the p47 subunit of the NADPH oxidase binds cooperatively to PtdIns(3)P and phosphatidic acid (16), and the vinculin tail co-ligates phosphatidylinositol 4,5-bisphosphate and PtdSer (15).

Although it is becoming evident that insertion of proteins into membranes is widespread, the three-dimensional orientations and quantitative binding properties remain challenging to characterize. The most common electron paramagnetic resonance and fluorescence approaches have provided important insights (17–20) but require covalent attachment of paramagnetic groups to various positions of the protein or mutations of residues. The inevitable effects of these modifications on lipid interactions indicate a need to develop new methods that provide quantitative measures of bilayer insertion by native proteins.

The early endosome antigen 1 (EEA1) protein represents a paradigm for understanding the actions of peripheral membrane proteins. Its FYVE domain specifically binds to PtdIns(3)P-enriched membranes, docking EEA1 to early endosomes and facilitating fusion of vesicular membranes (7–9). This zinc-stabilized module is found in 29 human proteins and has been engineered into an intracellular probe having nanomolar PtdIns(3)P affinity (21, 22). Three-dimensional structures of the FYVE domains of EEA1 (13, 23), Hrs (24), and Vps27 (25) proteins have been solved. Despite the structural similarity, different models of their membrane orientations have been inferred, emphasizing the need for experimentally derived estimates of membrane insertion.

Here we present a multivalent mechanism of membrane binding and insertion by the EEA1 FYVE domain based on structural and quantitative analysis of its lipid and micelle

[1] The abbreviations used are: PI, phosphoinositide; PtdIns(3)P, phosphatidylinositol 3-phosphate; PtdSer, phosphatidylserine; EEA1, early endosome antigen 1; NOESY, nuclear Overhauser effect spectroscopy; HSQC, heteronuclear single quantum coherence; DPC, dodecylphosphocholine; DHPC, diheptanoyl phosphatidylcholine; MIL, membrane insertion loop.

interactions. Information was gathered by several solution state NMR methods, including the use of spin-labeled lipid probes incorporated at various locations within the micelle. The paramagnetic spin labels broaden the NMR resonances of lipid-inserted residues in an established distance-dependent fashion (26–28), allowing a model of the micelle complex to be derived. The affinity of the FYVE domain for PtdIns(3)P, PtdSer, and several micelle systems revealed remarkable synergy within the multivalent complex that is responsible for early endosome recognition.

EXPERIMENTAL PROCEDURES

Protein Purification—The FYVE domain of human EEA1 (residues 1325–1410) was cloned into a pGEX-KG vector (Amersham Biosciences), expressed in *Escherichia coli* BL21 (DE3) pLysS in M9 medium supplemented with zinc sulfate, $^{15}NH_4Cl$ and $^{13}C_6$-glucose, or LB medium, and purified as previously described (13, 29). The protein was concentrated into 20 mM d_{11}-Tris, pH 6.8, in the presence of 200 mM KCl, 20 mM perdeuterated dithiothreitol, 50 μM 4-amidinophenylmethane sulfonyl fluoride, and 1 mM NaN_3, in either 5% or 99.99% $^2H_2O/H_2O$.

NMR Spectroscopy—NMR spectra of samples containing 0.2–1 mM unlabeled or uniformly ^{15}N- and $^{15}N,^{13}C$-labeled FYVE domain, 0–5 mM C_4-PtdIns(3)P, 0–1.5 mM C_{16}-PtdIns(3)P (Echelon Biosciences Inc.), 0–250 mM d_{38}-DPC (Cambridge Isotopes), 0–25 mM protonated DPC, and 0–30% w/w 1,2-dicaproyl-*sn*-glycero-3-[phospho-L-serine] (PtdSer) (Avanti) were recorded at 25 °C on Varian INOVA 500 and 600 MHz spectrometers. Intermolecular and intramolecular NOEs were obtained from ^{13}C F_1-filtered, F_2-edited nuclear Overhauser effect spectroscopy (NOESY) (30), ^{15}N-edited NOESY-HSQC (31), and ^{13}C-edited NOESY-HSQC (32) spectra with mixing times (τ_m) of 50–200 ms. The $J_{HNH}\alpha$ coupling constants were derived from $^1H,^{15}N$ HMQC-J and HNHA spectra (32).

Lipid Binding Properties—Lipid binding was characterized by monitoring chemical shift changes in the $^1H,^{15}N$ HSQC spectra of 200–250 μM FYVE domain as C_4-PtdIns(3)P was added stepwise to 1.8 mM, DPC to 500 mM (or 8.4 mM micellar), CYFOS-4 (Anatrace) to 250 mM (12.5 mM micellar), or DHPC (Avanti) to 300 mM (2.3 mM micellar). Micellar concentration corresponds to the solution concentration of intact micelles and is obtained by dividing the value of a detergent molecular concentration by an average aggregation number. The K_D values were calculated by a nonlinear least squares analysis using the Xmgr program and the equation $\Delta\delta = (\Delta\delta_{max}L)/(K_D + L)$, where L is the concentration of a lipid, and $\Delta\delta_{max}$ is the difference in the chemical shifts of the free and bound protein, respectively. Aggregation numbers for DPC, DHPC, and CYFOS-4 micelles were estimated by pulsed field gradient NMR methods (33) to be 56, 130, and 20 molecules, consistent with previous studies (34). The intensity profiles were standardized against those obtained for DPC micelles (34) and cytochrome *c* under similar conditions.

Paramagnetic Spin Labels—The 5- and 14-doxyl derivatives of 1-palmitoyl-2-stearoyl-*sn*-glycero-3-phosphocholines (3–6 mM) (Avanti) were added stepwise to 250 μM ^{15}N-labeled FYVE domain in the presence of 1.25 mM C_4- or C_{16}-PtdIns(3)P, 0–10% PtdSer, and 250 mM d_{38}-DPC. The $^1H,^{15}N$ HSQC spectra were collected for each point, and the intensities of backbone amide resonances were compared. Significant levels of intensity reduction were judged to be greater than the average plus one standard deviation and were confirmed by comparison with the line broadening in similar experiment when PtdIns(3)P was absent. The final ratio of spin label to micelle was between 0.7 and 1.3. The spin labels did not alter the protein structure based on the absence of chemical shift perturbations.

Synthesis of a Spin-labeled Derivative of PtdIns(3)P and Its Interaction with the FYVE Domain—The D(+)-1-*O*-[1-[6-(3-carboxy-PROXYL)-amino]hexanoyl]-2-palmitoylglyceryl D-myo-phosphatidylinositol 3-phosphate free radical (**3**) was synthesized as shown in Fig. 5*a*. The *N*-hydroxysuccinimidyl-3-carboxylate proxyl, free radical (**2**) (5.3 mg, 18.7 μmol) in *N,N*-dimethylformamide (0.5 ml) was added to D(+)-1-*O*-[1-(6-aminohexanoyl)]-2-palmitoylglyceryl D-myo-phosphatidylinositol 3-phosphate (**1**) (6.1 mg, 7.3 μmol) in 0.25 M tetraethylammonium bromide (TEAB) buffer (0.5 ml, pH 7.8) and stirred overnight at room temperature. The reaction mixture was concentrated to dryness, and the residue was washed with acetone (5 × 1.5 ml). The crude product was dissolved in water and applied to a DEAE cellulose column (12 × 15 mm). The product (**3**) was eluted with 0.2–2.0 M TEAB and 3:7 MeOH: TEAB, lyophilized, dissolved in water, stirred with DOWEX 50X8–200

(K^+ form) resin for 1 h, and filtered, and the filtrate was lyophilized yielding the product as the potassium salt (5.2 mg; matrix-assisted laser desorption ionization mass spectrometry: m/z = 931.9 [M-H, free acid]$^{1-}$).

Interaction of the FYVE domain with derivative **3** was monitored by collecting $^1H,^{15}N$ HSQC spectra of the 300 μM ^{15}N-labeled FYVE domain in the presence of 1.5 mM C_{16}-PtdIns(3)P and 250 mM d_{38}-DPC, whereas the 6-proxyl compound **3** was added stepwise up to 4.5 mM. Reduction of the backbone amide signal intensity for each residue was plotted as a histogram.

RESULTS AND DISCUSSION

Depth of Micelle Insertion—Five complementary approaches were used to estimate the depth of micelle insertion by the EEA1 FYVE domain. First, a spin-labeled "depth" probe was used to identify the most deeply buried residues of the FYVE domain (Fig. 1*a*). This 14-doxyl phosphatidylcholine derivative contains a doxyl moiety attached to the fourteenth position of the stearoyl chain. It spontaneously incorporates into DPC micelles and broadens the NMR signals of nuclei that are typically 10–12 bonds away from the micelle head groups (26–28). When the 14-doxyl probe was added to the ^{15}N-labeled FYVE domain that had been prebound to C_{16}-PtdIns(3)P and perdeuterated DPC micelles, a substantial reduction of the Val^{1366}, Thr^{1367}, and Val^{1368} amide signal intensities was observed (Fig. 1, *a* and *e*). Consequently, these three residues, which correspond to a conserved hydrophobic protrusion in the FYVE domain, are buried most deeply in the micelle core and constitute the membrane insertion loop (MIL). Insertion of the Val^{1366} and Thr^{1367} side chains into the micelle was confirmed by contacts observed in isotope-filtered and edited NOESY spectra. Nineteen intermolecular NOE cross-peaks were detected between the resonances of DPC and the Val^{1366}-Thr^{1367} sequence of the $^{13}C,^{15}N$-labeled FYVE domain complexed with C_4-PtdIns(3)P (Fig. 2). The methylene resonances of the DPC dodecyl group exhibited the strongest intermolecular NOE correlations to the Val^{1366} and Thr^{1367} side chains, indicating the insertion of these MIL residues in the hydrophobic core of DPC micelles. The insertion of Val^{1366} and Thr^{1367} into the micelle was also apparent from the reduction of their solvent exchange rates. Titration of DPC micelles into the C_4-PtdIns(3)P-bound FYVE domain specifically decreased intensity of the cross-peaks between the water and Val^{1366} and Thr^{1367} amide resonances in ^{15}N-edited NOE spectra (data not shown), indicating the reduced exposure of these residues to solvent. Despite the inherent mobility within protein micelle complexes (36), the intermolecular NOE and the line broadening data suggest that the MIL is the primary point of insertion of the domain into the hydrophobic micelle interior.

The mode of micelle insertion is robust, not being significantly affected by micelle size. We compared three phospholipids that share the same zwitterionic phosphatidylcholine head group that predominates in mammalian membranes but differ in their acyl chains. In aqueous solutions these lipids form micelles that mimic the membrane environment and are well suited for NMR studies (36). The micelles formed by cyclohexylbutylphosphocholine (CYFOS-4) or DHPC are approximately three times smaller (6.3 kDa) and larger (62.6 kDa), respectively, than d_{38}-DPC micelles (21.8 kDa) based on translational diffusion co-efficients measured by pulsed field gradient (33) NMR studies. Upon the addition of either phospholipid to the PtdIns(3)P-bound FYVE domain, the protein amide resonances exhibited very similar changes, with the largest chemical shift perturbations observed for the Val^{1366} and Thr^{1367} residues. This is consistent with the dramatic change in the environment of these residues upon insertion and indicates a common mode of penetration into the hydrophobic interior despite differences in the hydrophobic packing, surface pressure, size, and curva-
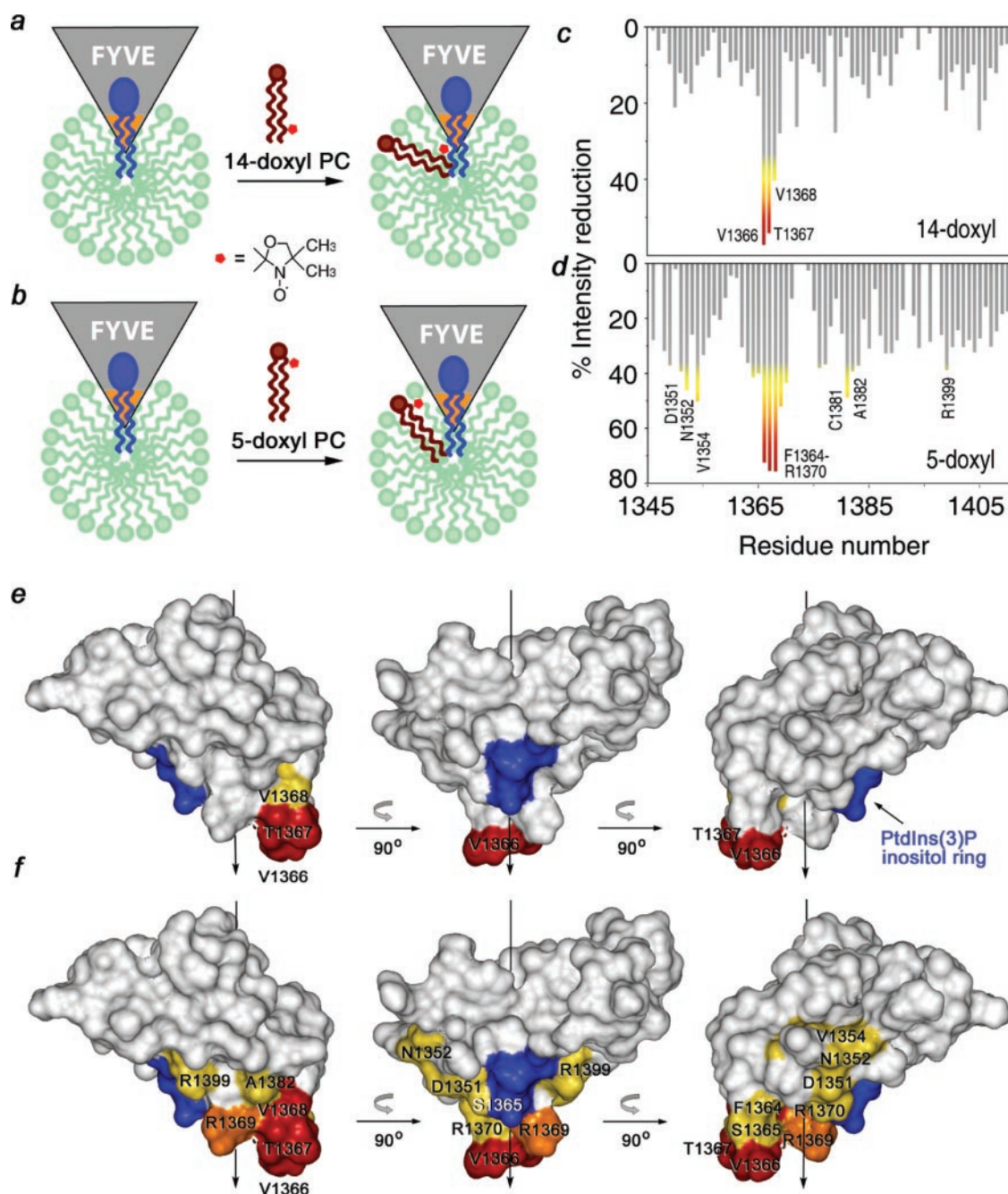
FIG. 1. **Depth and angle of PtdIns(3)P-bound FYVE domain insertion into micelles.** The addition of 14-doxyl (*a*) and 5-doxyl (*b*) probes (*red*) to the ^{15}N-labeled FYVE domain (*gray triangle*) prebound to C_{16}-PtdIns(3)P (*blue*) and d_{38}-DPC micelles (*green*) results in the loss of signal intensities in the MIL residues (*orange*). The histograms show reduction of intensity in the backbone amide resonance of each residue induced by the addition of 14-doxyl (*c*) and 5-doxyl (*d*). The colored bars indicate significant changes, being greater than the average plus one standard deviation. The FYVE domain surface colored *red*, *orange*, and *yellow* depicts residues that exhibit significant signal intensity reductions upon addition of 14-doxyl (*e*) and 5-doxyl (*f*). Three perspectives that rotate 90° about the axis of membrane insertion (depicted as a *vertical arrow*) are shown.

ture of the micelle systems. These results also suggest that the principles of micelle insertion revealed here may be extrapolated to bilayer interactions.

The functional importance of the MIL is underscored by mutagenesis studies. Replacement of Val[1366] and Thr[1367] by Gly or Glu residues abolishes the subcellular localization of EEA1 (29). Alanine substitution of the corresponding Leu[185] and Leu[186] residues of Vps27p or Phe[20] of Hrs decreases the affinities of their FYVE domains for PtdIns(3)P-containing vesicles by factors of 7 and 20, respectively (37). Thus, this hydrophobic protrusion appears to represent a general point of membrane insertion among FYVE domains.

Deep and stable insertion into the membrane requires PtdIns(3)P. In the absence of this ligand, small but significant chemical shift changes are seen in the MIL upon the addition of DPC, suggesting a weak micelle interaction that resembles the stronger PtdIns(3)P-dependent insertion (13). However, selective broadening of the MIL resonances was not observed upon titration of the 5- or 14-doxyl spin labels into the PtdIns(3)P-free state of the micelle-saturated FYVE domain (data not shown). Consequently, the nonspecific micelle association of the EEA1 FYVE domain is relatively superficial or transient. Similarly, PtdIns(3)P is needed for the FYVE domains of Hrs and Vps27p to insert sufficiently into phospholipid monolayers
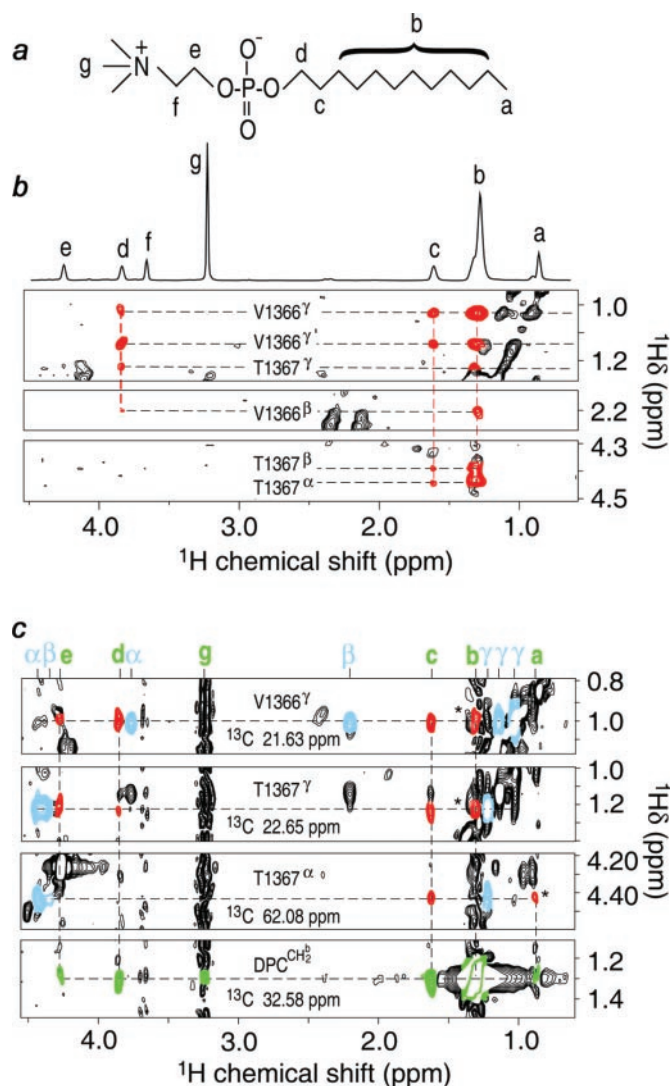
FIG. 2. **Micelle interactions with the PtdIns(3)P-bound FYVE domain.** *a*, the structure of DPC is shown, and hydrogen atoms are labeled. *b*, regions of a ^{13}C F$_1$-filtered, F$_2$-edited NOESY spectrum (τ_m = 200 ms) of 1 mM ^{13}C,^{15}N-labeled FYVE domain in the presence of 5 mM C$_4$-PtdIns(3)P and 25 mM protonated DPC are shown. Intermolecular NOEs between the α, β, and γ protons of Val[1366] and Thr[1367] residues and H^b, H^c, and H^d of DPC are shown in *red*. The ^{1}H spectrum of DPC is depicted above. The DPC resonances are labeled according to the positions indicated in *a*. *c*, strips from the ^{13}C-edited NOESY spectrum (τ_m = 135 ms) of 1 mM ^{13}C,^{15}N-labeled FYVE domain in the presence of 5 mM C$_4$-PtdIns(3)P, 5 mM protonated DPC and 245 mM d$_{38}$-DPC are depicted. Intermolecular NOEs between protein and DPC are colored *red*. Intramolecular NOEs of the FYVE domain and DPC are *blue* and *green*, respectively. Ambiguous NOE peaks are denoted with an *asterisk*.

to disrupt the surface pressure (37). Although the nonspecific membrane association is weak, it could serve to concentrate protein near bilayers and correctly position FYVE domains for PtdIns(3)P ligation.

Interestingly, the depth of FYVE domain insertion appears to be independent of the time scale of PtdIns(3)P contact. That is, the MIL resonances were similarly broadened by the 14-doxyl probes in the micelle-saturated FYVE domain bound to either dibutanoyl (C$_4$) or dipalmitoyl (C$_{16}$) PtdIns(3)P (Fig. 1*c* and Supplementary Fig. 1). The longer chain PtdIns(3)P interacts more tightly with the FYVE domain, exhibiting slow exchange on the NMR time scale, whereas the short chain form was in intermediate exchange (Fig. 3, *a* and *b*). Thus, the shorter residency time of the protein on the micelle did not substantially compromise the depth of insertion.

Angle of Micelle Insertion—To further define the membrane orientation of the FYVE domain, the angle of insertion was investigated. The surface of the domain buried within the micelle was identified using a "shallow" 5-doxyl probe (Fig. 1*b*). This phosphatidylcholine derivative carries the nitroxyl radical at the 5 position of the stearoyl chain and broadens resonances of nuclei that are located one to three bonds away from the lipid phosphates (26–28). The 5-doxyl probe was added to the ^{15}N-labeled FYVE domain that had been prebound to the C$_{16}$-PtdIns(3)P-containing DPC micelles. This resulted in the reduction of NMR signal intensities within the MIL and surrounding residues located at the level of the PtdIns(3)P head group, including Asp[1351], Asn[1352], Val[1354], Phe[1364]–Arg[1370], Cys[1381], Ala[1382], and Arg[1399] (Fig. 1*d*). These residues form a continuous surface of the FYVE domain that was used to derive the angle and extent of micelle insertion (Fig. 1*f*).

The vector that defines the orientation of the micelle inserted FYVE domain was estimated by optimizing the average position of the 5-doxyl radical relative to the micelle-bound protein. All the significant intensity reductions caused by paramagnetic line broadening were used in Newton minimization to satisfy the experimental distance restraints. The vector of FYVE domain insertion into PtdIns(3)P-containing DPC micelles (shown in Fig. 1*f*) differs from the molecular axis by an angle of 48°. The estimation of the insertion vector is consistent with the chemical shift (13) and mutagenesis data (29) and yields a model of the inserted state, in which the hydrophobic protuberance of the FYVE domain and the surrounding exposed polar residues maximize complementary contacts with the interior and interfacial zones of the micelle, respectively.

Electrostatic Interactions Alter the Angle of Insertion—The extensive interface between the FYVE domain and micelle head groups suggests additional stabilizing lipid interactions. Mammalian early endosomes are enriched in PtdSer, an acidic phospholipid that comprises ~8.4% of the total lipid (38). To determine whether electrostatic contacts contribute to targeting the FYVE domain to PtdIns(3)P-containing membranes, we investigated its interaction with PtdSer. Titration of soluble dicaproyl (C$_6$)-PtdSer into the FYVE domain, which had been prebound to C$_{16}$-PtdIns(3)P and DPC micelles, caused significant chemical shift changes in residues located in and around the MIL and the site of PtdIns(3)P coordination (Fig. 4, *a* and *b*). These perturbations indicated that PtdSer interactions involve the contiguous polar residues Arg[1369], His[1371], Glu[1383], and Lys[1387], which form a predominantly basic patch (Supplementary Fig. 2) that could easily accommodate a PtdSer head group next to a bound PtdIns(3)P molecule. Conservation of the basic residues and frequent substitution of a basic residue for Glu[1383] (Supplementary Fig. 3) suggest that this electrostatic interaction is a common feature among FYVE domains.

Interaction with PtdSer changed the estimated angle of insertion by ~25° and increased the affinity of the FYVE domain for PtdIns(3)P-containing micelles (see below). That is, when the 5-doxyl probe was added to the FYVE domain bound to micelles containing C$_6$-PtdSer, C$_{16}$-PtdIns(3)P, and DPC, the micelle insertion angle was estimated to be ~73°, based on decrease of the amide resonance intensities, in contrast to an angle of ~48° in the absence of PtdSer (Fig. 4, *c* and *d*). This orientation tilts the FYVE domain such that the PtdSer site interacts more extensively with the micelle, slightly exposing the opposite face containing the hinge and N-terminal mobile element. The PtdSer-stabilized orientation nearly aligns the FYVE domain with the micelle surface and is more similar to that suggested by the crystal structure of the EEA1 dimer (23), and by computer modeling (39), thus providing a unifying
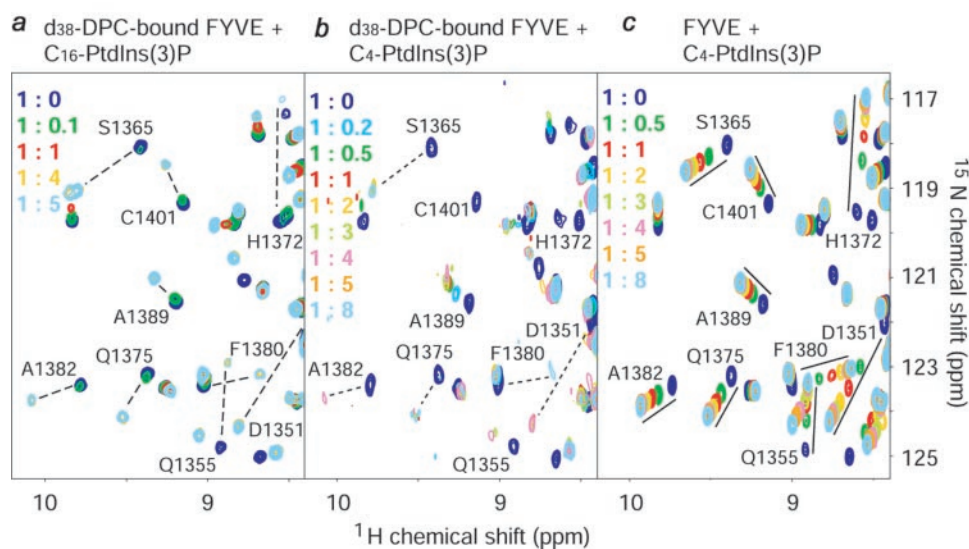
FIG. 3. **Superposed ¹H, ¹⁵N HSQC spectra of the FYVE domain reveal slow (*a*), intermediate (*b*), and fast (*c*) exchange regimes for the interactions with C₁₆-PtdIns(3)P-containing d₃₈-DPC micelles, C₄-PtdIns(3)P-containing d₃₈-DPC micelles, and C₄PtdIns(3)P, respectively.** The relative concentrations of the ¹⁵N-labeled FYVE domain (200 μM) and PtdIns(3)P are *inset* and color-coded. *a* and *b* were obtained in the presence of 250 mM d₃₈-DPC.

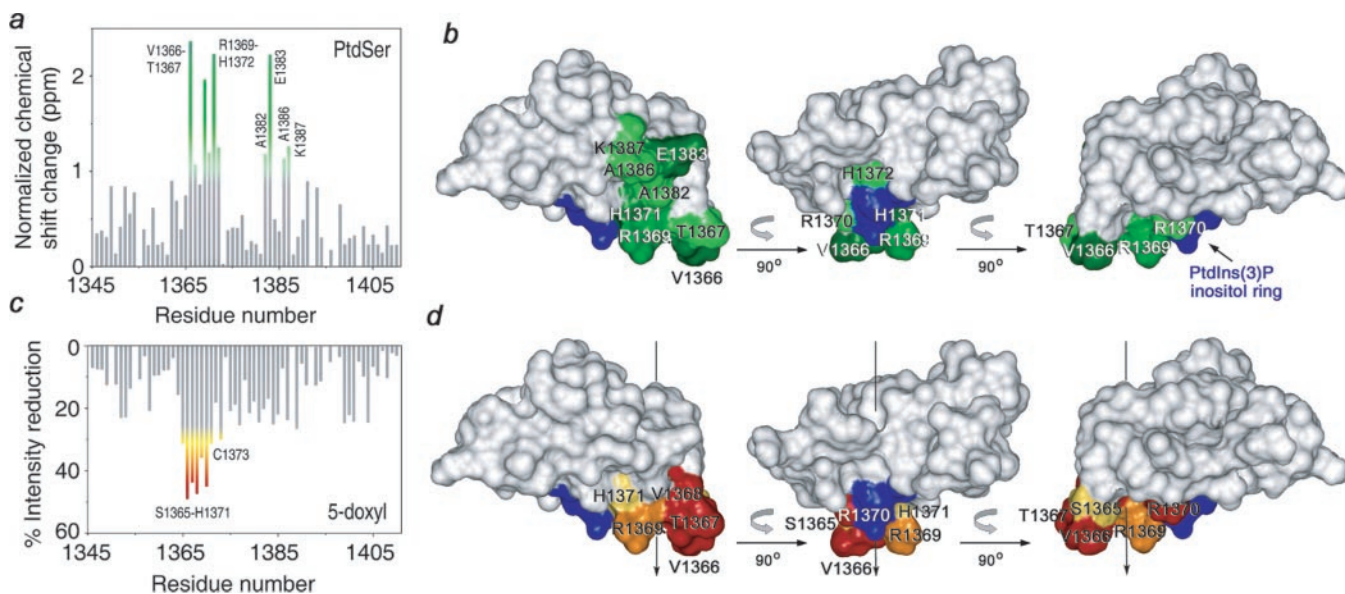FIG. 4. **Interactions of the FYVE domain with PtdSer-containing micelles.** *a*, the histogram shows normalized ¹⁵N,¹H chemical shift changes (52) of backbone amides of the FYVE domain (200 mM) complexed with C₁₆-PtdIns(3)P (1 mM) and DPC (250 mM) upon titration of C₆-PtdSer (up to 30% w/w). *b*, residues that exhibit significant PtdSer-induced resonance perturbations (more than the average plus one standard deviation) in *a* are labeled and colored in shades of *green* on the FYVE domain surface. *c*, the histogram shows the intensity of reduction in the FYVE domain backbone amide signals induced by the 5-doxyl probe incorporated into DPC micelles containing C₁₆-PtdIns(3)P and 10% PtdSer. Observed changes are colored in gradations of *red, orange, yellow*, and *gray* for large, medium, small, and insignificant, respectively. *d*, the residues that exhibit significant reduction of intensity in *c* are labeled and colored in *red, orange*, and *yellow* on the FYVE domain surface. The insertion axis is shown as a *vertical vector* in the three orthogonal views.

mechanism for the range of previously proposed insertion modes (23, 25).

Orientation of PtdIns(3)P Acyl Chains—To determine position of the PtdIns(3)P acyl chains in the FYVE domain complex, a novel spin-labeled phosphoinositide derivative was synthesized (Fig. 5*a*). This compound carries a proxyl radical at the C₆ position of the first acyl chain (40, 41). The addition of an equimolar amount of the proxyl PtdIns(3)P to the FYVE domain, which had been prebound to C₁₆-PtdIns(3)P and DPC micelles, resulted in the line broadening of several amide resonances, most significantly those of the Val¹³⁶⁶-Thr¹³⁶⁷ sequence (Fig. 5, *b* and *c*). These data indicate that the proxyl group, which may be mobile, is on average positioned nearest the MIL. Residues on either side of the inositol ring, such as

Glu¹³⁵⁰–Asn¹³⁵² and Arg¹³⁹⁹, also exhibited line broadening, consistent with their proximity to the PtdIns(3)P acyl chains. The lack of discernible NOEs between the PtdIns(3)P acyl chains and the FYVE domain suggests that such spin label restraints represent a feasible approach for characterizing the interactions between the acyl chains of the ligand and the micelle-inserted protein.

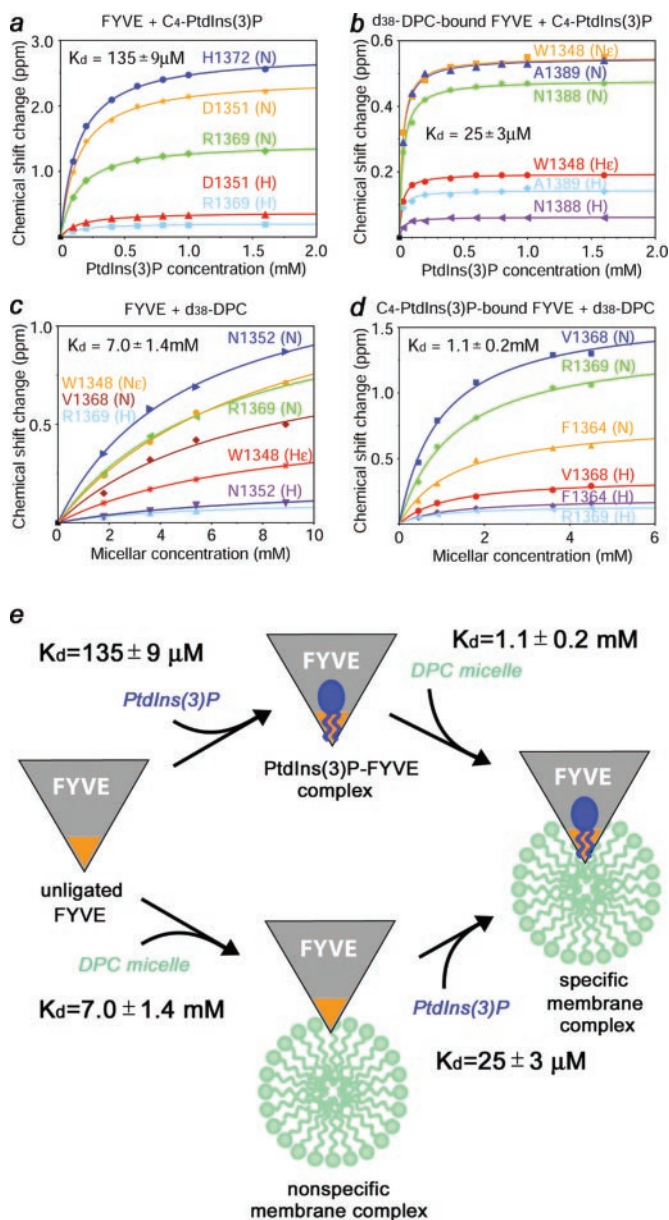*Conformational Changes*—The dramatic change in chemical environment upon membrane insertion of a protein suggests the potential for conformational change. Indeed, ligation of soluble PtdIns(3)P triggers the N-terminal hinge of the FYVE domain to move toward the lipid-binding site to coordinate the inositol ring, yielding a more globular closed conformation (13, 23). This conformational change buries an N-terminal Trp¹³⁴⁸
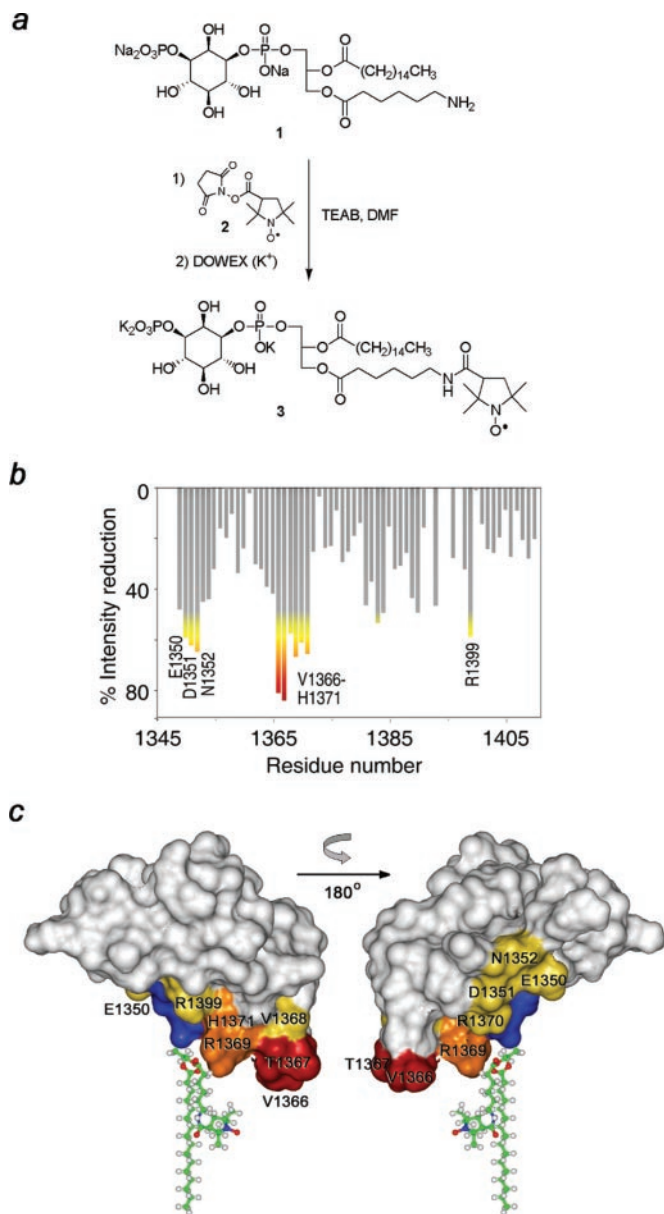
FIG. 5. **Orientation of PtdIns(3)P acyl chains.** *a*, synthesis of the proxyl PtdIns(3)P (**3**) from the proxyl (**2**) and PtdIns(3)P (**1**) compounds is shown, as described under "Experimental Procedures." *b*, the histogram displays a loss of amide signal intensities in the HSQC spectra caused by the addition of proxyl PtdIns(3)P (**3**) to the ^{15}N-labeled FYVE domain in the presence of C_{16}-PtdIns(3)P and d_{38}-DPC micelles. Significant changes are colored. *c*, the residues that exhibit significant intensity reduction in *b* are labeled and colored in *red*, *orange*, and *yellow* on the FYVE domain surface. The lipid acyl chains are shown as ball-and-stick models with carbon, oxygen, nitrogen, and hydrogen atoms colored *green*, *red*, *blue*, and *light gray*, respectively, and are oriented parallel to the insertion axis.

FIG. 6. **Affinities of the FYVE domain for PtdIns(3)P and micelles.** Titration of C_4-PtdIns(3)P (*a* and *b*) and d_{38}-DPC (*c* and *d*) into the FYVE domain induces changes in the backbone and Trp indole ^{15}N and ^{1}H resonances, as observed in HSQC spectra. The ^{15}N-labeled FYVE domain was initially either unbound (*a* and *c*), d_{38}-DPC-associated (*b*), or C_4-PtdIns(3)P-bound (*d*). The estimated binding affinities are *inset*. *e*, a model of sequential interactions of the FYVE domain with C_4-PtdIns(3)P or DPC micelles involve the indicated monovalent affinities, the product of which yields a predicted bivalent affinity of 160 nM.

residue, based on the blue shift of its fluorescence emission wavelength from 350 to 338 nm (Supplementary Fig. 4) and the emergence of new intramolecular NOEs (13). Further evidence for induced structure in the hinge and N-terminal mobile element was drawn from changes in backbone angles and chemical shifts (Supplementary Figs. 5 and 6) and from hydrogen bonds formed between Asp[1351] and the inositol ring (23). In addition, the Val[1366]-Thr[1367] resonances became substantially broadened upon the addition of C_4-PtdIns(3)P to the free FYVE domain, suggesting changes in local dynamics.

In contrast to the substantial conformational changes induced by PtdIns(3)P ligation, micelle interaction has a small, albeit significant, effect. In the absence of PtdIns(3)P, nonspecific micelle association is accompanied by chemical shift changes not only in the MIL but also in residues of the hinge and N-terminal mobile element (Fig. 6*c* and Supplementary Fig. 6). Furthermore, these ^{1}H and ^{15}N resonance perturbations were generally opposite in direction to those observed upon PtdIns(3)P ligation, suggesting that nonspecific micelle interaction may favor the open state of the PtdIns(3)P-binding site. On the contrary, the structure of the PtdIns(3)P-bound FYVE domain was essentially unchanged upon insertion, based on the similarity of the intramolecular NOE patterns observed in the presence or absence of micelles (Fig. 2 and Supplementary Fig. 7) and negligible chemical shift perturbations detected outside the vicinity of membrane insertion (13).

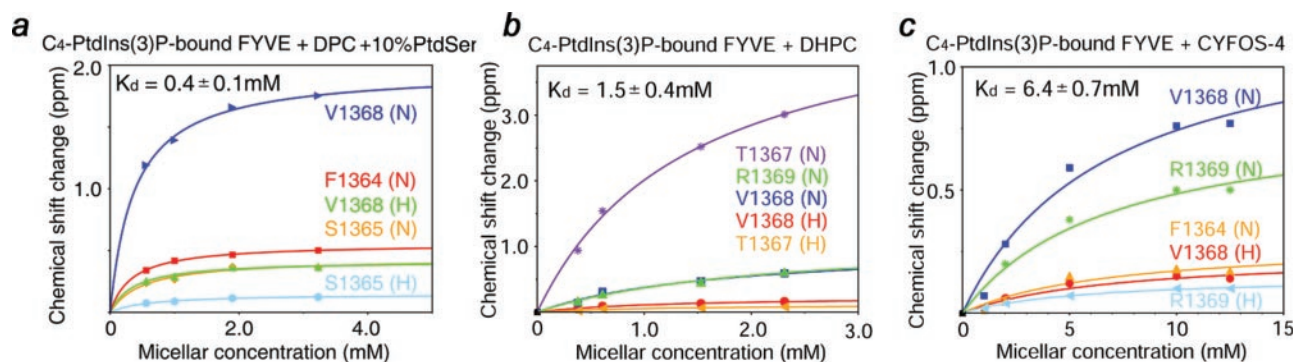*Affinities of Membrane Component Interactions*—The re-

FIG. 7. **Micelle affinities of the FYVE domain.** Titration of 10% C_6-PtdSer/90% d_{38}-DPC (*a*), DHPC (*b*), and CYFOS-4 (*c*) induces perturbations of the backbone amide resonances in HSQC spectra of the C_4-PtdIns(3)P-bound FYVE domain. The estimated binding affinities are labeled.

cruitment of peripheral proteins to membrane often involves interactions with multiple lipid head groups. Here, affinities of the FYVE domain for several lipids that represent major components of the early endosome membrane were investigated. Dibutanoyl PtdIns(3)P was bound by the free FYVE domain with a K_D of 135 ± 9 μM, as determined from chemical shift perturbation analysis (Fig. 6*a*). However, interaction with the same ligand in the presence of DPC micelles was 5.4 times stronger, yielding an affinity of 25 ± 3 μM (Fig. 6*b*). This binding enhancement presumably reflects the increased local concentration of the protein and PtdIns(3)P on the micelle surface in orientations that promote their interaction.

Similar enhancement is exerted by PtdIns(3)P on the micelle interactions of the FYVE domain. That is, the d_{38}-DPC micelle affinity of the free FYVE domain was approximately six times weaker (7.0 ± 1.4 mM) than that of the C_4-PtdIns(3)P-bound FYVE domain (1.1 ± 0.2 mM; Fig. 6, *c* and *d*). This may be explained by a preference for the exposed acyl chains of the bound PtdIns(3)P molecule to become buried inside a micelle. Accordingly, extending the PtdIns(3)P acyl chains or increasing the MIL hydrophobicity is likely to enhance this interaction. Indeed, the micelle-associated FYVE domain bound more tightly to the C_{16} form than the C_4 form of PtdIns(3)P, as evidenced by their slow and intermediate exchange on the NMR time scale, respectively (Fig. 3). The bivalent affinity of the FYVE domain for C_4-PtdIns(3)P-containing micelles, estimated as a product of the two sequential binding events (42), is then predicted to be ~160 nM (Fig. 6*e*), approaching the 50 nM affinity of EEA1 for liposomes (21, 43). The estimates of the binding affinity and chemical shift perturbations for small, medium, and large micelles suggested a similar mode of micelle insertion. In particular, the affinities of C_4-PtdIns(3)P-loaded FYVE domain for d_{38}-DPC, DHPC, and CYFOS-4 micelles were 1.1 ± 0.2, 1.5 ± 0.4, and 6.4 ± 0.7 mM, respectively, as calculated using micellar concentrations (Fig. 7, *b* and *c*), indicating that these interactions are largely independent of micelle size.

Further stabilization of the FYVE domain-micelle complex is provided by the electrostatic engagement of PtdSer. The interaction of C_4-PtdIns(3)P-complexed FYVE domain with DPC micelles containing 10% C_6-PtdSer was significantly stronger than its interaction with the DPC micelles alone, yielding a K_D of 0.44 ± 0.1 mM (Fig. 7*a*). When multiplied by the PtdIns(3)P affinity, this infers a mulivalent affinity of ~70 nM, closely matching the 50 nM affinity of full-length EEA1 for PtdIns(3)P-containing liposomes (21, 43), as well as the ~42 and ~75 nM affinities of the Hrs and Vps27p FYVE domains for PtdIns(3)P-containing monolayers (37). The dimerization of EEA1 through its central coiled coil region may further increase membrane affinity of the protein by juxtaposing a pair of FYVE domains (23). However, the isolated EEA1 FYVE domain is monomeric and contributes only weakly to the EEA1 dimer interface seen

by x-ray crystallography (23). In agreement with these results, we found that the FYVE domain appears to be monomeric when associated with equimolar PtdIns(3)P and excess DPC micelles, based on its translational diffusion co-efficient. This corroborates the dimerization-independent membrane recruitment of Hrs FYVE domain (44) and emphasizes the fact that the monomeric FYVE domain is the fundamental unit of membrane recognition through its synergistic lipid interactions.

In conclusion, the FYVE domain membrane docking mechanism described here involves (i) specific PtdIns(3)P binding, (ii) insertion of a hydrophobic loop into the bilayer, and (iii) stabilizing electrostatic interactions with acidic phospholipids.

The crystal and solution structures of the EEA1 FYVE domain clearly demonstrate how PtdIns(3)P is bound (13, 23). Three motifs coordinate the PtdIns(3)P molecule: the N-terminal W*XX*D, the central R(R/K)HHCRXCG, and C-terminal RVC sequences. Recognition of the phosphate groups of the lipid is mediated by Arg and His residues in the central R(R/K)HHCRXCG basic motif, whereas Asp^{1351} and His^{1372} provide stereospecificity by forming hydrogen bonds to the hydroxyl groups of the inositol ring. All three motifs are remarkably conserved in the FYVE sequences and comprise the canonical phospholipid coordination site. The critical roles of the PtdIns(3)P binding residues have been confirmed by alanine substitution experiments. Mutation of the conserved residues in the signature motifs abolishes binding or reduces the affinity for PtdIns(3)P-containing membranes, yielding proteins with diffuse cytosolic distributions (43).

The residues that insert into the micelle are also conserved among FYVE domains in terms of hydrophobicity and proximity to the PtdIns(3)P site, suggesting similar mechanism of membrane insertion and synergy with PtdIns(3)P ligation. The Hrs and Vps27 proteins contain FTFTN and FSLLN sequences in place of the FSVTV sequence of EEA1, and these exposed loops occupy similar conformations (24, 25). Moreover, mutations of the MIL residues of EEA1, Hrs, and Vps27p disrupt the localization of these proteins to membranes or decrease membrane affinity, revealing a crucial role for this element in membrane association (29, 37).

The PtdSer interaction of the EEA1 FYVE domain is likely to contribute to the recruitment of the protein to PtdIns(3)P-embedded membranes. Conservation of the basic residues of EEA1 in the PtdSer site and frequent introduction of an additional Lys or Arg residues in the corresponding regions of other FYVE domains indicate that electrostatic contacts with negatively charged membrane surfaces are a common feature. The FYVE domain interaction with acidic membrane lipids other than PtdSer not only enhances the membrane affinity but also stabilizes a more interfacially active orientation where the PtdIns(3)P molecule is sandwiched between the domain and membrane. Likewise, membrane binding of p40^{phox} and

p47^{phox} PX domains (16, 45), ENTH domains of Epsin1 and the analogous ANTH domain of AP180 (46), and the PH domain (47, 48) of phospholipases C-δ, C-γ, and C-β (49) is enhanced by the nonspecific electrostatic contacts with acidic lipids in membranes.

Together, these elements provide the overall affinity and lipid specificity necessary for precise targeting of FYVE domain-containing proteins to early endosomes. The FYVE domain of EEA1 binds to soluble dibutanoyl PtdIns(3)P with an affinity of 135 μM. Stabilization caused by insertion into DPC micelles provides a net affinity of ~160 nM, with PtdSer further enhancing binding by a factor of 2.5 and yielding a ~70 nM affinity. This closely matches the 50 nM affinity that was estimated for dipalmitoyl PtdIns(3)P-containing acidic liposomes (21, 23, 43). Other FYVE domains are recruited to membranes containing PtdIns(3)P and acidic lipids with comparable affinities. The FENS-1 protein exhibits a 48 nM affinity for liposomes containing PtdIns(3)P, and similar binding is displayed by its isolated FYVE domain (50). The interaction of PIKfyve with PtdIns(3)P-containing liposomes is shown to be mediated by the FYVE domain and involves an affinity of at least 550 nM (51). The FYVE domains of *Drosophila* Hrs and Vps27p have affinities of 42 and 75 nM, respectively, for monolayers which contain PtdIns(3)P (37). Overall, these data suggest a general mechanism of the FYVE domain docking to PtdIns(3)P-enriched membranes, which involves a substantial network of interactions that determine PtdIns(3)P specificity, hydrophobic insertion, and nonspecific electrostatic stabilization.

REFERENCES

1. Murray, D., Ben-Tal, N., Honig, B., and McLaughlin, S. (1997) *Structure* **5,** 985–989
2. Bhatnagar, R. S., and Gordon, J. I. (1997) *Trends Cell Biol.* **7,** 14–20
3. Overduin, M., Cheever, M. L., and Kutateladze, T. G. (2001) *Mol. Interventions* **1,** 150–159
4. Lee, E., Marcucci, M., Daniell, L., Pypaert, M., Weisz, O. A., Ochoa, G. C., Farsad, K., Wenk, M. R., De Camilli, P., and Gaedigk, A. (2002) *Science* **297,** 1193–1196
5. Zimmermann, P., Meerschaert, K., Reekmans, G., Leenaerts, I., Small, J. V., Vandekerckhove, J., David, G., and Gettemans, J. (2002) *Mol. Cell* **9,** 1215–1225
6. Stolt, P. C., Jeon, H., Song, H. K., Herz, J., Eck, M. J., and Blacklow, S. C. (2003) *Structure* **11,** 569–579
7. Burd, C. G., and Emr, S. D. (1998) *Mol. Cell* **2,** 157–162
8. Gaullier, J. M., Simonsen, A., D'Arrigo, A., Bremnes, B., Stenmark, H., and Aasland, R. (1998) *Nature* **394,** 432–433
9. Patki, V., Lawe, D. C., Corvera, S., Virbasius, J. V., and Chawla, A. (1998) *Nature* **394,** 433–434
10. Perisic, O., Fong, S., Lynch, D. E., Bycroft, M., and Williams, R. L. (1998) *J. Biol. Chem.* **273,** 1596–1604
11. Ford, M. G., Mills, I. G., Peter, B. J., Vallis, Y., Praefcke, G. J., Evans, P. R., and McMahon, H. T. (2002) *Nature* **419,** 361–366
12. Seelig, A., Blatter, X. L., Frentzel, A., and Isenberg, G. (2000) *J. Biol. Chem.* **275,** 17954–17961
13. Kutateladze, T. G., and Overduin, M. (2001) *Science* **291,** 1793–1796
14. Cheever, M. L., Sato, T. K., de Beer, T., Kutateladze, T. G., Emr, S. D., and Overduin, M. (2001) *Nat. Cell Biol.* **3,** 613–618
15. Johnson, R. P., Niggli, V., Durrer, P., and Craig, S. W. (1998) *Biochemistry* **37,** 10211–10222
16. Karathanassis, D., Stahelin, R. V., Bravo, J., Perisic, O., Pacold, C. M., Cho, W., and Williams, R. L. (2002) *EMBO J.* **21,** 5057–5068
17. Kohout, S. C., Corbalan-Garcia, S., Gomez-Fernandez, J. C., and Falke, J. J. (2003) *Biochemistry* **42,** 1254–1265
18. Frazier, A. A., Wisner, M. A., Malmberg, N. J., Victor, K. G., Fanucci, G. E., Nalefski, E. A., Falke, J. J., and Cafiso, D. S. (2002) *Biochemistry* **41,** 6282–6292
19. Perisic, O., Paterson, H. F., Mosedale, G., Lara-Gonzalez, S., and Williams, R. L. (1999) *J. Biol. Chem.* **274,** 14979–14987
20. Chapman, E. R., and Davis, A. F. (1998) *J. Biol. Chem.* **273,** 13995–14001
21. Gillooly, D. J., Morrow, I. C., Lindsay, M., Gould, R., Bryant, N. J., Gaullier, J. M., Parton, R. G., and Stenmark, H. (2000) *EMBO J.* **19,** 4577–4588
22. Kutateladze, T. G., and Overduin, M. (2003) in *Handbook of Metalloproteins* (Messerschmidt, A., ed) Vol. 3, John Wiley & Sons, Ltd., Chichester, UK
23. Dumas, J. J., Merithew, E., Sudharshan, E., Rajamani, D., Hayes, S., Lawe, D., Corvera, S., and Lambright, D. (2001) *Mol. Cell* **8,** 947–958
24. Mao, Y., Nickitenko, A., Duan, X., Lloyd, T. E., Wu, M. N., Bellen, H., and Quiocho, F. A. (2000) *Cell* **100,** 447–456
25. Misra, S., and Hurley, J. H. (1999) *Cell* **97,** 657–666
26. Papavoine, C. H., Konings, R. N., Hilbers, C. W., and van de Ven, F. J. (1994) *Biochemistry* **33,** 12990–12997
27. Van Den Hooven, H. W., Spronk, C., Van De Kamp, M., Konings, R. N. H., Hilbers, C. W., and Van De Ven, F. J. M. (1996) *Eur. J. Biochem.* **235,** 394–403
28. Jarvet, J., Zdunek, J., Damberg, P., and Graslund, A. (1997) *Biochemistry* **36,** 8153–8163
29. Kutateladze, T. G., Ogburn, K. D., Watson, W. T., de Beer, T., Emr, S. D., Burd, C. G., and Overduin, M. (1999) *Mol. Cell* **3,** 805–811
30. Zwahlen, C., Legault, P., Vincent, S. J. F., Greenblatt, J., Konrat, R., and Kay, L. E. (1997) *J. Am. Chem. Soc.* **119,** 6711–6721
31. Marion, D., Kay, L. E., Sparks, S. W., Torchia, D. A., and Bax, A. (1989) *J. Am. Chem. Soc.* **111,** 1515–1517
32. Ikura, M., Kay, L. E., Tschudin, R., and Bax, A. (1990) *J. Magn. Reson.* **86,** 204–209
33. Altieri, A. S., Hinton, D. P., and Byrd, R. A. (1995) *J. Am. Chem. Soc.* **117,** 7566–7567
34. Lauterwein, J., Bosch, C., Brown, L. R., and Wuthrich, K. (1979) *Biochim. Biophys. Acta* **556,** 244–264
35. Chen, J., Feng, L., and Prestwich, G. D. (1998) *J. Org. Chem.* **63,** 6511–6522
36. Henry, G. D., and Sykes, B. D. (1994) *Methods Enzymol.* **239,** 515–536
37. Stahelin, R. V., Long, F., Diraviyam, K., Bruzik, K. S., Murray, D., and Cho, W. (2002) *J. Biol. Chem.* **277,** 26379–26388
38. Kobayashi, T. (1998) *Nature* **392,** 193–197
39. Diraviyam, K., Stahelin, R. V., Cho, W., and Murray, D. (2003) *J. Mol. Biol.* **328,** 721–736
40. Prestwich, W. V. (1996) *Acc. Chem. Res.* **29,** 503–513
41. Rauch, M. E., Ferguson, C. G., Prestwich, G. D., and Cafiso, D. S. (2002) *J. Biol. Chem.* **277,** 14068–14076
42. Tochtrop, G. P., Richter, K., Tang, C., Toner, J. J., Covey, D. F., and Cistola, D. P. (2002) *Proc. Natl. Acad. Sci. U. S. A.* **99,** 1847–1852
43. Gaullier, J. M., Ronning, E., Gillooly, D. J., and Stenmark, H. (2000) *J. Biol. Chem.* **275,** 24595–24600
44. Sankaran, V. G., Klein, D. E., Sachdeva, M. M., and Lemmon, M. A. (2001) *Biochemistry* **40,** 8581–8587
45. Stahelin, R. V., Burian, A., Bruzik, K. S., Murray, D., and Cho, W. (2003) *J. Biol. Chem.* **278,** 14469–14479
46. Stahelin, R. V., Long, F., Peter, B. J., Murray, D., De Camilli, P., McMahon, H. T., and Cho, W. (2003) *J. Biol. Chem.* **278,** 28993–28999
47. Lemmon, M. A., and Ferguson, K. M. (2000) *Biochem. J.* **350,** 1–18
48. Lemmon, M. A., Ferguson, K. M., and Abrams, C. S. (2002) *FEBS Lett.* **513,** 71–76
49. Singh, S. M., and Murray, D. (2003) *Protein Sci.* **12,** 1934–1953
50. Ridley, S. H., Ktistakis, N., Davidson, K., Anderson, K. E., Manifava, M., Ellson, C. D., Lipp, P., Bootman, M., Coadwell, J., Nazarian, A., Erdjument-Bromage, H., Tempst, P., Cooper, M. A., Thuring, J. W., Lim, Z. Y., Holmes, A. B., Stphens, L. R., and Hawkins, P. T. (2001) *J. Cell Sci.* **114,** 3991–4000
51. Sbrissa, D., Ikonomov, O. C., and Shisheva, A. (2002) *J. Biol. Chem.* **277,** 6073–6079
52. Grzesiek, S., Stahl, S. J., Wingfield, P. T., and Bax, A. (1996) *Biochemistry* **35,** 10256–10261